Advanced non-invasive fluorescence spectroscopy and imaging for mapping photo-oxidative degradation in acrylonitrile–butadiene–styrene: A study of model samples and of an object from the 1960s

D. Comelli [a,*], F. Toja [b], C. D'Andrea [a,c], L. Toniolo [b], G. Valentini [a], M. Lazzari [d], A. Nevin [e]

[a] *Dipartimento di Fisica, Politecnico di Milano, Piazza Leonardo da Vinci 32, Milano 20133, Italy*
[b] *Dipartimento di Chimica, Politecnico di Milano, Via Mancinelli 7, Milano 20133, Italy*
[c] *Center for NanoScience and Technology CNST-IIT@POLIMI, via Pascoli 70/3, 20133 Milano, Italy*
[d] *Centre for Research in Biological Chemistry and Molecular Materials (CIQUS), University of Santiago de Compostela, 15782 Santiago de Compostela, Spain*
[e] *Istituto di Fotonica e Nanotecnologie - Consiglio Nazionale delle Ricerche (IFN-CNR), Dipartimento di Fisica, Politecnico di Milano, Piazza Leonardo da Vinci 32, Milano 20133, Italy*

Article history:
Received 20 September 2013
Received in revised form
15 December 2013
Accepted 23 December 2013
Available online 3 January 2014

1. Introduction

Much tangible Cultural Heritage is made of naturally occurring polymeric materials. Over the last century synthetic materials were introduced to the market and used for the creation of works of art, industrial and household objects, offering new forms of expression for artists, architects and designers [1,2]. Thus the degradation of modern synthetic materials is of particular interest to curators and collectors, archives and researchers – and understanding, preventing and monitoring chemical modifications which may alter the appearance and stability of plastics is crucial for the conservation of historical design objects [3]. Extensive research has been carried out to establish methods for analysis and characterisation of plastic objects, including recent studies on non-invasive analytical techniques based on the detection of volatile organic compounds (VOC) [4] and near infrared (NIR) [5,6] or terahertz (THz) imaging [7]. However, little research has concentrated on the direct analysis of the degradation of plastic objects and polymers using fluorescence-based techniques [8–10]. This work focusses on the application of non-invasive and advanced fluorescence spectroscopy and imaging for assessing photodegradation of model samples and a naturally degraded object made of acrylonitrile–butadiene–styrene (ABS), a polymer which has received limited scientific study in heritage collections [3].

While scientific analysis of historical objects made of ABS is limited [11], significant research has been dedicated to the study of the degradation and stability of the material which is widely used in industry [12–14]. ABS is a copolymer made of an acrylonitrile–styrene continuous phase (SAN) and partially grafted polybutadiene, the mechanical properties of which can be fine-tuned by varying grafting conditions and the proportions of components in the polymer. It is well known that ABS is prone to photo-oxidative degradation which

* Corresponding author. Tel.: +39 0223996165; fax: +39 0223996126.
E-mail addresses: daniela.comelli@polimi.it, danicomelli@gmail.com (D. Comelli).

may lead to chemical modifications such as crosslinking and chain scission and significant colour changes (yellowing) with the build-up of oxidation products and changes in the free volume of the blend [15,16]. The susceptibility of ABS to photo-oxidative degradation is due to the instability of butadiene, and in particular to the presence of residual double bonds along the polymer chains [17]. This degradation of ABS has been shown to involve an autocatalytic free radical chain mechanism where allylic radicals react with oxygen to form hydroperoxides products. Labile oxygen–oxygen bonds break to form RO• radicals, precursors of oxidation products identified in ABS such as aldehydes, esters, carboxylic acids and ketones [17–20].

Because of difficulties in sampling important historical design objects and the need for rapid methods for the assessment of chemical changes, non-invasive analytical methods, which can provide indications of the composition and degree of degradation of an object without requiring the taking of samples, are desirable [3]. Fluorescence spectroscopy is particularly suitable for the analysis of plastics as changes in fluorescence may be related to modifications in chemical composition; fluorescence spectroscopy, and in some cases fluorescence lifetime measurements, have been employed for the assessment of oxidation of polymers including polyethylene [8], polystyrene [21], styrene butadiene copolymers [22], and styrene ethylene butadiene styrene (SEBS) copolymers [23,24].

With respect to point-like analysis, imaging techniques can provide a rapid indication of the heterogeneous degradation and condition of plastic objects. More in detail, both spectroscopy imaging methods, including those based on the analysis of the NIR radiation reflected and absorbed by a surface [5,6], and structural imaging methods, based on THz techniques [7], have proved to be effective tools for monitoring degradation. In turn, fluorescence imaging, based on the analysis of the spectral [25,26] and lifetime [27] properties of the emission, has been used for the assessment of the conditions of cultural heritage and specifically paintings and sculptures, but has not been applied to the analysis of plastics or historical objects. Large multispectral imaging datasets can benefit from the application of supervised and unsupervised multivariate statistical methods, which can allow the discrimination of regions in an image on the basis of spectral differences, as has recently been established during investigations by means of NIR hyperspectral imaging [5,6,28].

In this work, standard samples of ABS were investigated under accelerated degradation conditions in which the processes occurring under natural conditions were provoked through accelerated photodegradation. Samples were studied using excitation-emission and time-resolved fluorescence spectroscopy to investigate changes in emission and fluorescence lifetime which occur with degradation. Non-invasive fluorescence spectroscopy, fluorescence multispectral and fluorescence lifetime imaging (FLIM) were then employed for the analysis of the complex three-dimensional (3D) surfaces of a well-known historical object made in ABS dating from 1965 – the Grillo telephone. Multivariate analysis of data from spectral images was applied to classify different areas of the object studied. Results from fluorescence analysis were compared with results from complementary analysis of micro-samples, collected from standard samples and from the object studied, by Fourier transform infrared spectroscopy (FTIR).

FTIR spectroscopy provides a method for identification of changes in bulk material due to modifications in FTIR spectra. However, the technique is inherently limited by its detection limit. Fluorescence spectroscopy, in contrast, may detect fluorescent oxidation products in trace concentrations before changes are apparent in FTIR spectra, but the interpretation of fluorescence spectra is less straightforward, as has been shown in another work on other polymer matrices [9].

2. Experimental

2.1. Reference ABS model samples and photodegradation

ABS reference materials were supplied as extruded rectangular blocks which were approximately 5 mm in thickness by Lanxess Srl, Milan. Accelerated photo-oxidative degradation mimiced natural degradation of ABS which has been shown to depend on the wavelength of irradiation, with different photo-oxidation mechanisms occurring below 300 nm [16]. For this reason, accelerated degradation is relevant even for objects stored indoors, although the comparison between accelerated degradation and natural ageing indoors is not trivial. Accelerated photodegradation of samples was carried out following the UNI 10925:2001 guidelines for artificial solar light testing [29] with the aid of a high-speed exposure unit (Suntest CPS+ apparatus, Heraeus, Germany), equipped with a Xenon lamp having a constant emittance of 765 W/m^2; a long-pass filter with cut-off wavelength at 295 nm was used to exclude radiation more energetic than that of outdoor solar exposure. The maximum temperature of the samples during irradiation was 45 °C in order to avoid any thermo-oxidative degradation. Samples of ABS were subjected to accelerated degradation with exposure to 5, 10, 50, 100, 200 500 and 1000 h.

2.2. Grillo telephone (1965)

An iconic design ABS object, the white Grillo folding telephone, was analysed. The object, designed in 1965 by Marco Zanuso and Richard Sapper and produced by Sit Siemens with a revolutionary and modern shape, is a recognisable precursor to the folding mobile telephone. Other telephones were also produced by Siemens in different vibrant colours of ABS. The white Grillo telephone analysed in this work (Fig. 1) is from a private collection and is no longer in use. The phone is made of four separate parts: the microphone and the dial with the speaker inside the internal part of the telephone and the two external encasing parts.

2.3. Fourier transform infrared spectroscopy (FTIR)

ABS reference samples and micro-samples taken from the Grillo telephone were analysed by FTIR. Micro-samples of less than 1×1 mm were taken from the edges of the object (considering both the internal and external sides of the telephone). Samples were analysed using a microdiamond ATR cell by placing small fragments under the objective, and bringing the sample stage in direct contact with the diamond surface. Pressure was regulated with the pressure sensor with which the Continuum microscope is equipped.

A Nicolet 6700 spectrophotometer equipped with a deuterated triglycine sulphate (DTGS) detector (between 4000 and 400 cm^{-1} with 128 acquisitions and 4 cm^{-1} resolution) was coupled with an attenuated total reflection diamond crystal accessory (ATR) or a Nicolet Continuum FTIR microscope equipped with an HgCdTe detector cooled with liquid nitrogen (acquired between 4000 and 700 cm^{-1}.) Spectra were baseline corrected using Omnic software and normalised on the basis of the intensity of the CN stretching vibration (2240 cm^{-1}).

2.4. Fluorescence excitation-emission spectroscopy

Fluorescence excitation-emission (EE) spectra were recorded with a Jobin-Yvon Fluorolog-3 Spectrofluorometer (HORIBA Ltd) equipped with a Xenon lamp, double excitation and single emission monochromators and a photomultiplier tube (PMT) detector. For this purpose, excitation was scanned between 250 and 500 nm and emission recorded between 280 and 750 nm; slits were fixed to

1 nm for the excitation monochromators and 5 nm for the emission monochromator. Maxima in fluorescence bands are listed as excitation wavelength (nm)/emission wavelength (nm). The detected signal was automatically corrected in order to obtain spectra independent from instrumental factors; for the purpose the spectral efficiency of the PMT detector and the spectral irradiance of the excitation lamp were taken into account. EE spectra are plotted as contour maps with 20 different levels of intensity from the maximum (red) to 10% of the minimum intensity (blue).

Measurements were performed on reference ABS samples employing a front-face collection mode. Points of interest on the surface of Grillo were analysed by using a custom-made fibre optic probe, made of two silica optical fibres of 1 mm core diameter (SFS1000 Fiberguide Industries) arranged in a 45°/0° configuration geometry; this geometry was chosen to minimise specular reflectance; moreover the position of fibres relative to the surface was adjusted to maximise the fluorescence intensity.

2.5. Time-resolved fluorescence spectroscopy

A time-resolved photo-luminescence (TRPL) system has been adapted to simultaneously measure the fluorescence lifetime at different emission wavelengths. The system is schematically based on a Streak camera detector, spectrometer and pulsed light source [27]. The latter is provided by a tuneable (680–1080 nm) Ti:Sapphire laser (Chameleon Ultra II, Coherent), which emits light pulses (pulse width of approximately 140 fs at the repetition rate of 80 MHz; laser power = 0.2 mW). Part of the beam is split off and directed to a photodiode in order to trigger the Streak camera. In order to select the desired excitation wavelength of 355 nm the laser beam is tuned to 710 nm and then frequency doubled by focussing it into a type I β-barium borate crystal. Finally, the frequency doubled optical signal is selected by means of short pass filters (Schott) and focused on the sample. The fluorescence signal is collected and focused on the entrance slit of the imaging spectrometer (focal length 300 mm, *f*/3.9, 50 lines/mm grating, Acton SP2300, Princeton Instruments), by two lenses ($f = 75$ mm and $f = 200$ mm, respectively; diameter = 50.8 mm). Between the two lenses a long-pass filter with cut-off at 400 nm (Comar Optics Inc.) is placed to select the fluorescence light. The spectrometer is coupled to a Streak camera detector (C5680, Hamamatsu) which works in synchroscan operation mode at 80 MHz. In this work we adopted the longest time range available in synchroscan mode (2 ns) which leads to a temporal resolution of about 20 ps. In order to evaluate the fluorescence amplitudes and lifetimes the decay profiles of interest have been fitted with a non-linear least square interpolation by means of the Curve Fitting Tool cftool (Matlab™). In this work a bi-exponential fitting function has been adopted.

2.6. Fluorescence imaging spectroscopy devices

Investigations on the Grillo telephone were conducted with two different portable fluorescence imaging devices to measure the spectral and temporal decay properties of the UV-induced fluorescence emissions from the plastic surface. Details of the two devices are described elsewhere [26,31] and are summarised here.

A multispectral camera, sensitive to the visible spectral range, is used to record fluorescence spectral information. The detector is made of a cooled monochrome CCD camera coupled with a band-pass liquid crystal tuneable filter. Fluorescence excitation is provided by two properly filtered low-pressure Mercury lamps (excitation wavelength ≈ 365 nm) leading to a typical mean irradiance of 200 μW/cm^2 on the analysed surface. The measurement protocol involves the acquisition of 33 luminescence images from 400 to 720 nm in 10 nm steps. After correction for the detector efficiency, the spectral shape of the emitted light in each point of the field of view can be estimated. As described elsewhere [26], refined analyses of spectral data include Principal Component Analysis (PCA) followed by fuzzy C-means clustering [32] performed on the most significant Principal Components (PCs).

Analysis of the temporal decay of the fluorescence emission is performed employing a FLIM system [27]. The detector is based on a nanosecond time-gated ICCD, whereas UV pulsed excitation is provided by a frequency-tripled diode-pumped Q-switch Nd–Yag laser, emitting 1 ns pulses at 355 nm. The laser beam is magnified with suitable optics in order to uniformly illuminate a circular area close to 25 cm in diameter, leading to a typical fluence per pulse kept below 140 nJ/cm^2 and to a typical mean irradiance below 14 μW/cm^2. Analysis of fluorescence time-resolved data implies the reconstruction of the effective lifetime map $\tau(x,y)$ in each point of the field of view assuming a simple mono-exponential decay [26].

3. Analysis of ABS reference samples

ABS reference samples were analysed to assess changes in fluorescence following photodegradation which resulted in visible yellowing of the samples, as has been reported by others [18]. In order to relate changes in fluorescence to molecular degradation, FTIR analysis was carried out on the same samples and is presented first. Detailed attributions of FTIR spectra are supplied in Supplementary information.

3.1. FTIR spectroscopy

FTIR spectra of the reference samples of ABS show the typical features of the constituting SAN (styrene–acrylonitrile) and PB (polybutadiene) phases (Fig. 2) [16,17].

Photodegradation of ABS induces readily detectable chemical modifications of the ABS. After 5 h of exposure to UV radiation, there is a decrease in the intensity of bands at 967 and 912 cm^{-1} ascribed to ω − CH of PB, and an increase in the band 3436 cm^{-1} from OH stretching – evidence of the formation of carboxylic acids and alcohols (see Table 1, Supplementary information). These are ascribed to the generation of free radicals (R and ROO•) following degradation of the photo-labile PB phase which may induce the

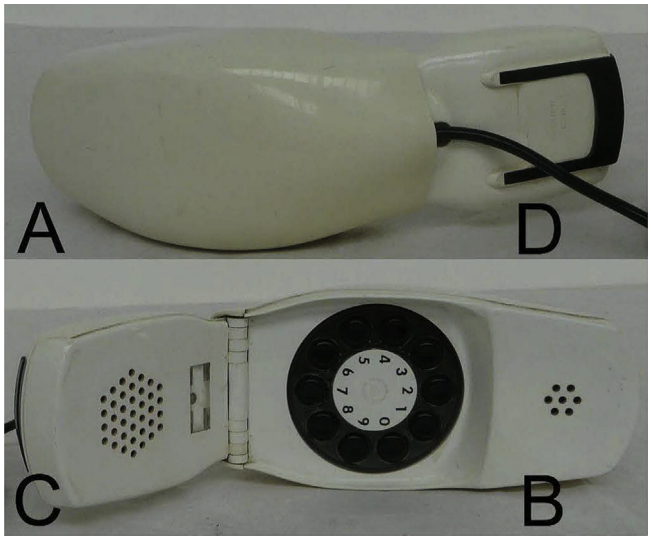

Fig. 1. The Grillo phone where the earpiece has an outer part (A) and an inner part (B). The microphone (C) is on the interior side of the folding phone which sits on the base (D) when closed.

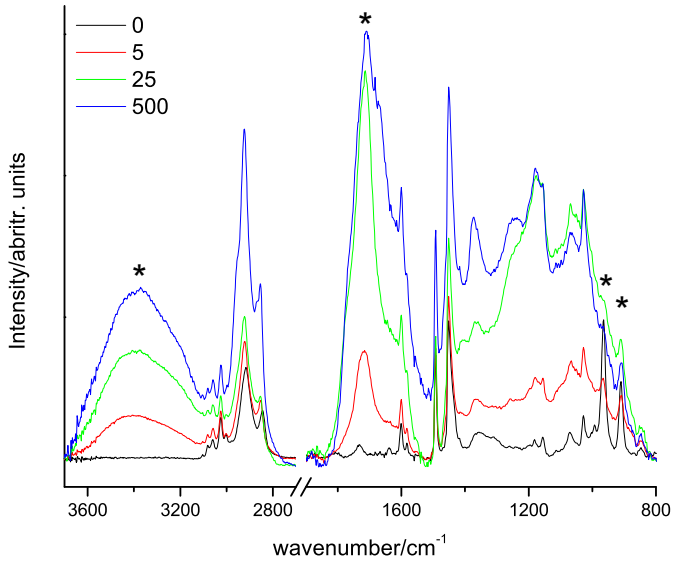

Fig. 2. FTIR spectra acquired from the surface of model samples of ABS as a function of the number of hours (0, 5, 25 and 500) of accelerated degradation; a significant increase in bands from O–H and C=O stretching (marked with an *) is observed due to the build-up of photo-oxidation products in the copolymer (see assignments and frequencies in Table 1, Supplementary information).

photo-oxidation of the PS units in the SAN phase [15]. The photo-oxidation of the PS leads to the formation of photo-oxidation products (α,β-unsaturated aldehydes, saturated ketones, and saturated aldehydes) that contribute to the broadening and increase in the intensity of the band ascribed to C=O stretching centred at 1720 cm^{-1} [33,34]. The examination of samples was irradiated for longer periods revealed increased oxidation of ABS with changes in intensity of the same bands.

3.2. Fluorescence excitation-emission spectroscopy

EE spectra highlight the presence of multiple fluorophores in ABS. Their attribution is made with reference to spectra reported for the analysis of polystyrene and other polystyrene copolymers which have been studied in greater detail [34,35]. Commercial ABS exhibits a principal band at 270–280/310 nm (Fig. 3(a)). While studies of PS fluorescence in copolymers containing polystyrene have suggested the formation of intramolecular excimers between neighbouring styrene rings which give rise to fluorescence emissions at 325–340 nm, the luminescence between 300 and 310 nm has been related to residual styrene molecules [21,35], or isolated styrene units or anomalous structures in the polymer [22,36,37]. It is likely that contributions from both isolated aromatic molecules and excimers give rise to the emission at 310 nm in ABS.

Fluorescence emissions from ABS following irradiation change significantly (Fig. 3(b) and (c)) and are summarised below. Changes in spectral shape reveal the formation of new fluorophores, and suggest modifications of the microenvironment surrounding fluorescent species in the material. Greatest modifications to fluorescence spectra occur following 5 h of exposure (Fig. 3(b)) to radiation of ABS which is accompanied by a slight yellowing of the materials. While the band at 280/310 nm decreases in intensity, another band appears at 310/350–450 nm, and a new, intense emission is observed at 365/480 nm.

Bands which appear following photodegradation are ascribed to photo-oxidation and the generation of degradation products which accumulate in the samples (including aromatic ketones), as supported by changes in FTIR spectra (Fig. 2). However, concentrations of fluorophores in ABS may be below the detection limit of FTIR (which is approximately 2% [11]); therefore the assignment of EE spectra proposed below is based on a comparison with emissions reported in analogous copolymers.

The reduction of the band at 280/310 may be related to charge-transfer from styrene to photo-oxidation products, as it has been observed in styrene–butadiene–styrene copolymers [22], and in the oxidation of other styrene copolymers [21]. Another competing factor contributing to the decrease in the intensity of the band is the reduction in the number of excimer sites due to chain scission and disaggregation of the styrene units, as has been observed in photo-oxidation of SEBS [23].

The band at 310/350–450 in ABS is more difficult to ascribe. Styrene oxidation leads to the formation of acetophenone (detected as a VOC) from ABS [4], a well-known fluorophore which Allen et al. attribute to the emission at 230/400–450 nm in irradiated SEBS [24]. Thus the band observed in ABS could be due to trapped acetophenone. Another assignment of this band is the generation of stilbene-like structures (with emissions at 370 nm, for example) [23].

Finally, the emission observed at 365/480 nm in ABS is similar to that reported following the irradiation of styrene–butadiene–styrene copolymers where the emission at 350/460 nm was ascribed to the development of α,β-unsaturated aldehydes or α,β diketones from the oxidation of PB [22].

After 25 h (Fig. 3(c)), the intensity of the band ascribed to styrene at 280/310 nm decreases and the intensity of the emission ascribed to α,β-unsaturated aldehydes or α,β diketones at 365/480 nm increases. The band at 310/350–450 (ascribed to volatile acetophenone) is no longer observed. With irradiation, and the generation of an increasing number of oxidation products, an emission in the visible at 435/500 nm develops, and there is a progressive bathochromic shift of the signal at 365/480 nm. A similar bathochromic shift in emission occurs when samples are excited at 355 nm (with a shift in the emission maximum from 435 (0 h) to 465 nm (after 25 h)).

3.3. Fluorescence lifetime spectroscopy

Time-resolved fluorescence spectroscopy provides additional evidence of molecular changes in ABS with irradiation. Following laser excitation at 355 nm the temporal properties of emissions between 400 and 470 nm ascribed to α,β-unsaturated aldehydes and α,β diketones were analysed and suggest that the fluorescence lifetime of the emission decreases with increasing exposure to radiation (see Table 2, Supplementary information). Specifically, standard ABS exhibits a bi-exponential fluorescence with lifetimes (and relative intensity) on order of 200 ps (27%) and 950 ps (75%). With extensive photodegradation, the lifetime reduces to 71 ps (38%) and 575 ps (62%). The shift in the picosecond fluorescence lifetimes suggests changes in the microenvironment surrounding the fluorophores and a modification of the fluorescent species which are present in the blend. The decrease in fluorescence lifetime with irradiation between 400 and 470 nm is similar to that reported in irradiated polyethylene films [8], which could be related to a change in the average molecular weight which has been shown to influence the lifetime of fluorophores in polystyrene [35].

4. Analysis of Grillo

The internal or unexposed surfaces of the Grillo telephone are white, while a moderate yellowing is observed on all the exposed surfaces (Fig. 1). The yellowing observed is ascribed to photo-oxidation of the ABS [18]. Below we present fluorescence imaging analyses followed by analysis using point-like fluorescence spectroscopy performed with fibre optics on points of interest of the object and by FTIR analysis performed on samples from the phone.

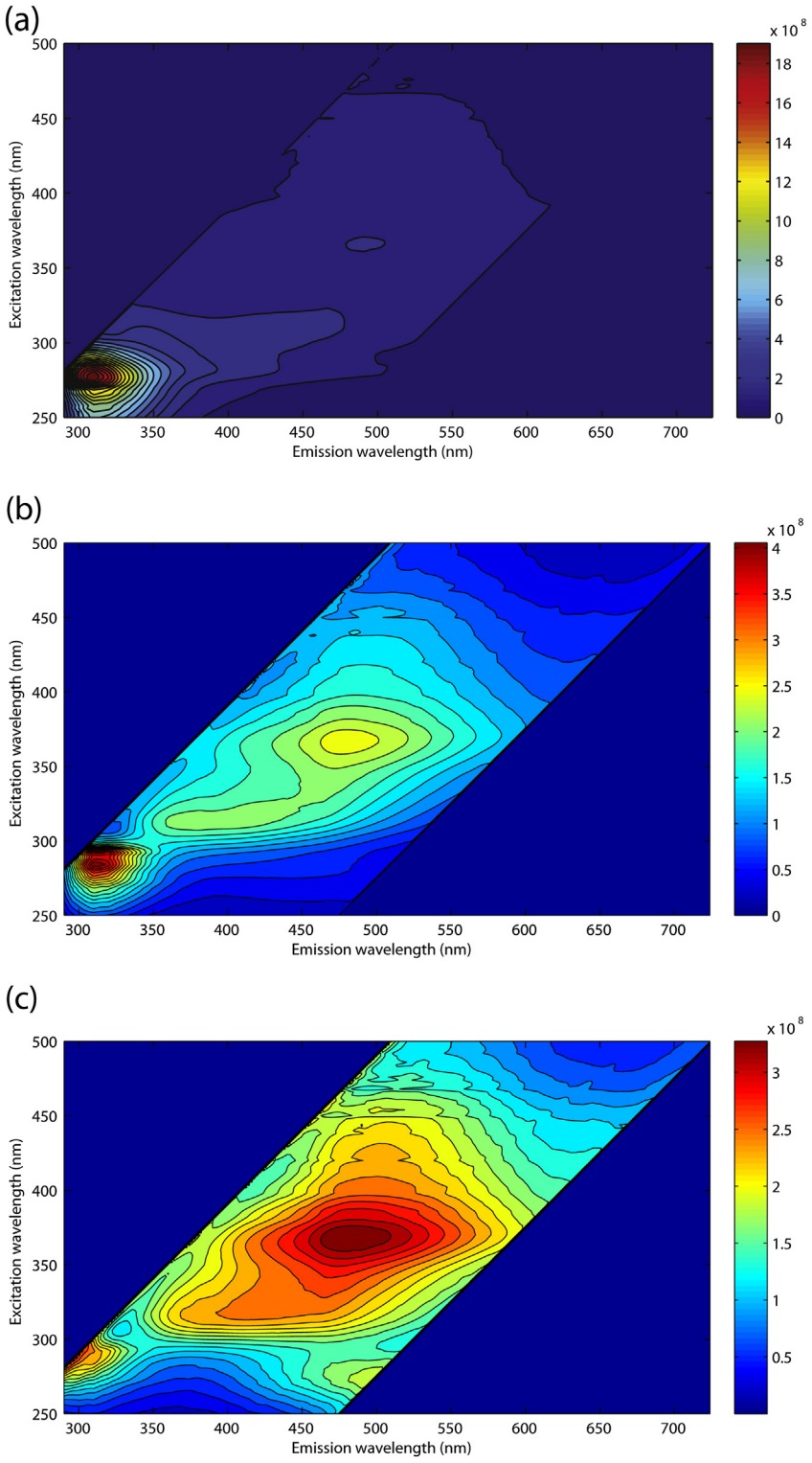

Fig. 3. EE spectra acquired from the surface of ABS exposed to (a) 0 h, (b) 5 h and (c) 25 h of irradiation. EE spectra are a matrix of emission spectra acquired at different excitation, where the most intense bands are shown in red as a function of excitation and emission wavelength. (For interpretation of the references to colour in this figure legend, the reader is referred to the web version of this article.)

4.1. Fluorescence multispectral imaging

As seen in the corrected RGB image, which represents the fluorescence emission of the faces of the object following excitation at 365 nm (Fig. 4), the internal and the external sides of the mouthpiece are associated with a bluish emission (with a maximum at 440 nm), while the other pieces of the phone have a blue–green (in the web version) emission (peaked at 490 nm). These spectral differences are ascribed to dissimilarities in the ABS formulations used for the various pieces (possibly containing optical brighteners, which are not present in the reference ABS material). Moreover, the fluorescence from the inner face of the

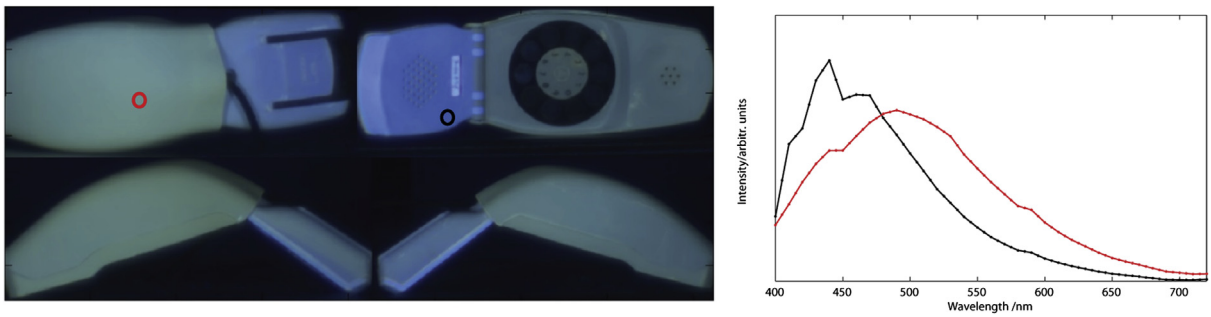

Fig. 4. (Left) Image of the colour of the emission following excitation at 365 nm reconstructed on the basis of the multispectral dataset of the different parts of the Grillo phone. (Right) Fluorescence spectra registered in correspondence of a point on the microphone (black line) and on the external encasing of the dial (red line). (For interpretation of the references to colour in this figure legend, the reader is referred to the web version of this article.)

earpiece appears slightly more blue than that observed from the top and the external sides. This last observation can be explained with reference to different exposure of the ABS plastic, the external parts of the phone being more exposed to ambient light and hence more affected by photodegradation.

For quantitative differentiation of areas of the object on the basis of fluorescence spectra, multivariate analysis of the spectral cube was carried out. Principal component analysis, performed on the covariance matrix, highlights differences in the image, as shown in the scatter plot of the first two PCs, which account for 99% of the variance of the dataset (Fig. 5).

From Fig. 5(a), it can be seen that the first two PCs chiefly separate the mouthpiece (subregions 1, 2 and 3) from the external and internal parts of the dial (subregions 4, 5 and 6). Moreover, in the scatter plot it is possible to observe a trend (highlighted by the two arrows in figure) correlated with areas of the phone characterised by increasing ambient exposure and hence greater degradation, which occurs on the top part of the external earpiece (subregion 4). Multivariate statistical analysis further suggests that the external left side (subregion 5) of the object is different from the right side (subregion 6), which we assume is a direct consequence of different levels of photodegradation.

Cluster analysis, performed on the first two PCs, provides another method for visualising the distribution of differences on the object which is separated into three groups (Fig. 6): the internal and external sides of the mouthpiece in green, surfaces from the inside of the receiver (less exposed to irradiation over time) in red (in the web version) and more exposed and likely more degraded surfaces in blue (in the web version). Fluorescence spectra registered in this last cluster are characterised by an emission which is bathochromically shifted with respect to spectra recorded in the second cluster. It has to be finally noticed that the result of the clustering method on the border of the phone is not trustworthy, due the low fluorescence signal detected on these areas.

4.2. Fluorescence lifetime imaging

FLIM images acquired on the different faces of the object are shown in a composite image in Fig. 7 and were calculated on the basis of the mean lifetime of the emission registered in the first 15 ns of decay in the visible spectral range between 400 and 700 nm. Roughly speaking, three different regions can be observed on the surface of the object, corresponding to an average lifetimes of 3.6 ns (the microphone in blue, in the web version), 4.1 ns (the bottom unexposed area of the base and the right exposed area of the earpiece, in yellow, in the web version), and 4.5 ns (the top and left exposed area of the earpiece and the dial and the speaker in the internal side, in red, in the web version). As inferred through previous multispectral fluorescence imaging analysis, the mouthpiece and the rest of the object are made of different ABS formulations.

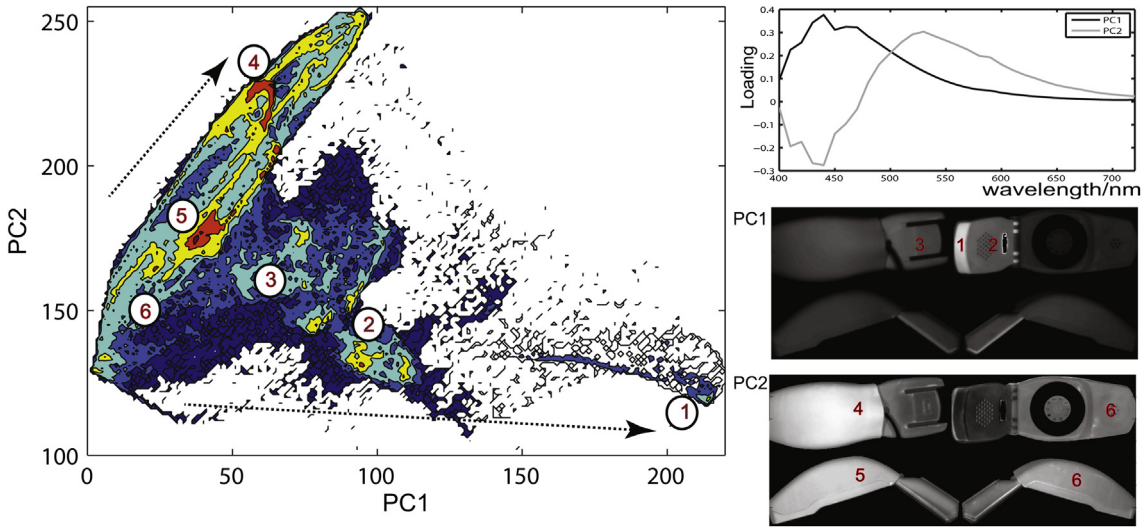

Fig. 5. (Left) Scatter plot of the first two PCs following multivariate analysis of the mosaicked multispectral image recorded from Grillo. Different areas of the phone are represented in different regions of the plot. Arrows indicate trends which are ascribed to areas of greater exposure to light. (Right) Loading functions and score maps of the first two PCs.

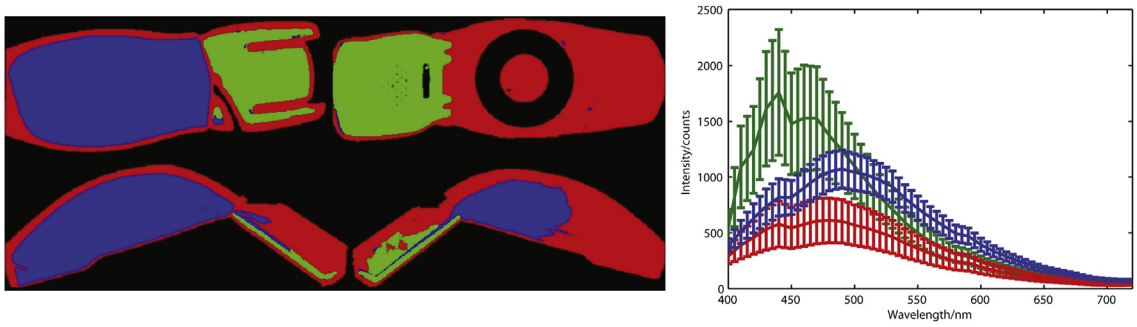

Fig. 6. (Left) Image of the Grillo phone subdivided into 3 clusters on the basis of fuzzy C-means clustering performed on the first two PCs of the multispectral dataset; black pixels refers to areas not included in the analysis. (Right) Mean fluorescence spectra and related standard deviation registered in each cluster.

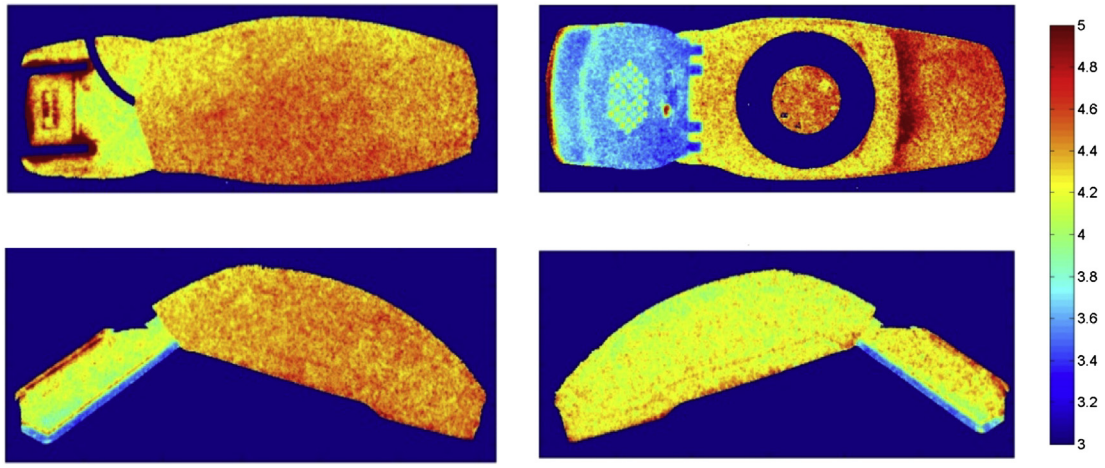

Fig. 7. Nanosecond fluorescence lifetime images of the different faces of the Grillo telephone.

These variations in formulation lead to the observation of different lifetimes in the two parts of the object (the shortest lifetime, close to 3.6 ns, on the internal side of the mouthpiece and the longest one, close to 4.5 ns, on the top exposed area of the earpiece and on the speaker in the internal side). Nevertheless, fluorescence lifetime seems to be even more sensitive than spectral emission properties to modifications which occur in ABS and its additives following degradation. For example, the mouthpiece is characterised by different lifetime in the top and bottom sides, most probably as a consequence of a different degradation of the polymer. This higher sensitivity can be explained with the strong dependence of emission lifetime to the microenvironment of fluorophores in ABS.

In other areas of the telephone (the earpiece and its external encasing part, which are made of single pieces of ABS), differences mapped with FLIM are again ascribed to the heterogeneous chemical modifications and accumulation of degradation products on the surface of the object. For example, in good agreement with multispectral analysis, the left and right sides of the earpiece, made of the same piece of ABS, are characterised by distinct lifetime properties which we ascribe to different degrees of exposure (4.5 ns and 4.1 ns for the left and right side, respectively).

With respect to lifetime analysis of reference ABS samples (measured with a streak camera-based device), nanosecond time-resolved fluorescence imaging suggests that more exposed areas (as the top exposed surface of the earpiece) are associated with an increase in the emission lifetime. The different results obtained with the two time-resolved devices suggest that FLIM analysis, performed on the first 15 ns of the decay emission kinetic, is more sensitive to long-living fluorophores produced by degradation phenomena. The lifetimes measured on reference ABS samples and on the Grillo phone are indeed attributed to emissions from different fluorescent species, including impurities and possibly additives introduced in the Grillo blend which differ from the reference ABS samples.

4.3. Fluorescence excitation-emission spectroscopy

EE spectra of model ABS samples (Fig. 3) and EE spectra acquired with a fibre optic probe from the Grillo telephone (Fig. 8(a)–(c)) are different, which confirms a difference in formulation, the presence of impurities and possibly the introduction of additives in Grillo. EE spectra collected from the internal sides and from the protected areas of the object (the base of the telephone, Fig. 8(a)) are dominated by an intense emission centred at 420/475–500 nm. The two weak bands detected at 260/300 nm and at 260/440 nm are tentatively ascribed to styrene molecules and acetophenone, respectively.

Significant differences in the shape of emissions are observed in EE spectra acquired from exposed (Fig. 8(c)) and unexposed areas (Fig. 8(b)). Indeed, the dominant broad fluorescence detected from exposed areas of Grillo is centred at 435/500 nm, bathochromically shifted with respect to the narrow emission observed in protected areas inside the phone, and similar to the band in the same position in photodegraded ABS which is ascribed to α,β-unsaturated aldehydes or α,β diketones. Results from fibre optic fluorescence spectroscopy are well correlated with multispectral analysis of the entire object and suggest that oxidation products are heterogeneously distributed on the object.

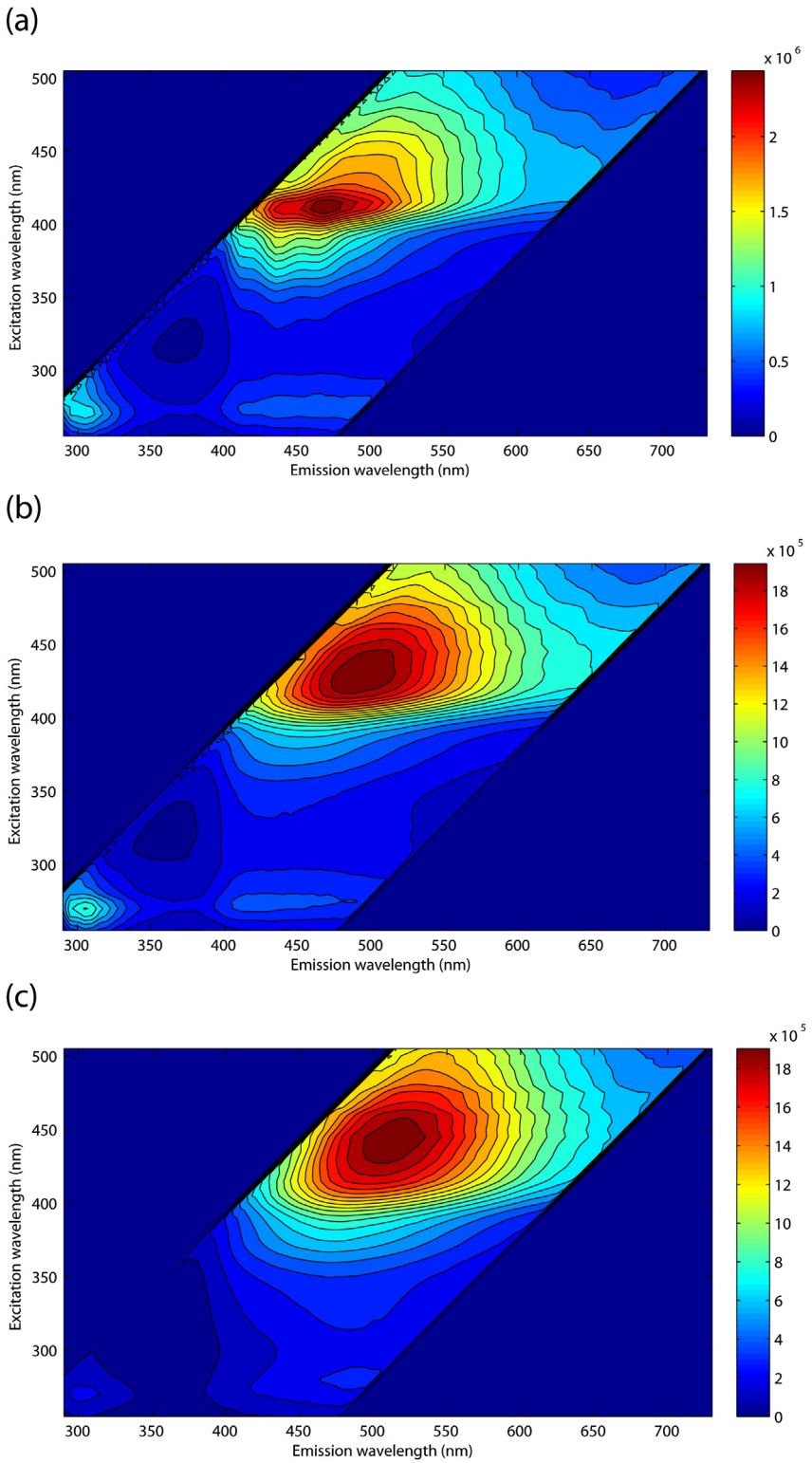

Fig. 8. EE spectra acquired from the surface of the Grillo telephone - (a) the base of the telephone (see Fig. 1D), (b) the inner surface of the earpiece (Fig. 1B) and (c) the outer surface of the earpiece (Fig. 1A).

In the specific case of Grillo, fluorescence imaging and fluorescence spectroscopy suggest that this object may be a composite re-assembled telephone: the mouthpiece is made of a formulation of ABS which has a different fluorescence lifetime and different fluorescence spectra from those observed on the other surfaces of the phone. While the reassembly of composite objects by dealers and in museums is common due to the problematic conservation of serial design objects, this practice compromises the integrity of these complex and culturally significant objects.

4.4. FTIR analysis of micro-samples from Grillo

FTIR of micro-samples confirmed the presence of ABS in all areas of the telephone, with main differences in samples related to the degree of degradation of the polymer. It was not possible to identify additives on the basis of the spectra acquired.

The photo-oxidative degradation of ABS in Grillo is apparent by comparing FTIR spectra collected on samples taken from the exposed left and right sides of the earpiece and unexposed surface (Fig. 9). Exposed areas present bands related to the formation of hydroxyl groups and significant accumulation of unsaturated and saturated aldehydes and are similar in terms of the intensity of C═O vs. C—C stretching (at approximatively 1720 cm^{-1} and 1640 cm^{-1}, respectively) to the ABS irradiated for 5 h. The complex shape of the telephone and exposure to uneven sources of light (for example exposure in a room where light is incident on one side of the telephone instead of the other) lead to differences in the spatial distribution and degree of degradation on the surface, as confirmed by fluorescence multispectral imaging, FLIM and fluorescence spectra collected from individual points; indeed FTIR from samples collected from the surface of the right and left sides of the earpiece of the phone suggest slight differences in the oxidation of the polymer, with greater signal from C═O and O—H stretching on left side of the earpiece, indicating a relatively greater build-up of degradation products. This result, with slight differences in the FTIR spectra from the two sides of the earpiece, confirms the modification observed with multispectral fluorescence imaging and FLIM of variations in the fluorescence emission and lifetime on the earpiece.

5. Conclusions

The integration of non-invasive fluorescence spectroscopy with advanced imaging based on fluorescence spectra and lifetime provides new insights into the photo-oxidation of ABS. Multivariate analysis as well as fluorescence lifetime imaging is fundamental for the visualisation of differences in fluorescence found on 3D objects. These methods highlight heterogeneous degradation in ABS models and in the historical Grillo telephone which can be related to the accumulation of fluorescent photo-oxidation products. Photodegradation and the build-up of chromophores may compromise the appearance of the object and have significant implications for the display of objects made in ABS in museum collections: the yellowing of ABS due to photo-oxidation is indeed a significant problem for the display of historical objects which have not been stabilised with the UV stabilisers commonly used today. Indeed the role of colourants and additives in ABS on changes on the degradation of the material still require further research. Because of the difficulty in the attribution of fluorescence spectra and results from fluorescence lifetime images to specific molecular changes, complementary analytical methods like FTIR spectroscopy or non-invasive Raman Spectroscopy can be used to directly assess the build-up of specific oxidation products. Our results demonstrate that, despite the challenges in spectral and lifetime interpretation, fluorescence spectroscopy and imaging can provide rapid and sensitive methods for the assessment of the distribution of changes in photo-oxidation.

Methods for the monitoring of the degradation of design objects in ABS like Grillo are needed, and could be based on an integration of results from point-like and imaging analyses. While practical solutions for the display of ABS without UV irradiation could limit the accumulation of photo-oxidation products, there are still no cleaning methods available to remove the yellowing effects observed in ABS without damage to the shiny surfaces. Therefore future research should focus on the assessment of additives in historical objects, the distribution of degradation products as a function of depth, and the investigation of new methods for the treatment of degraded objects.

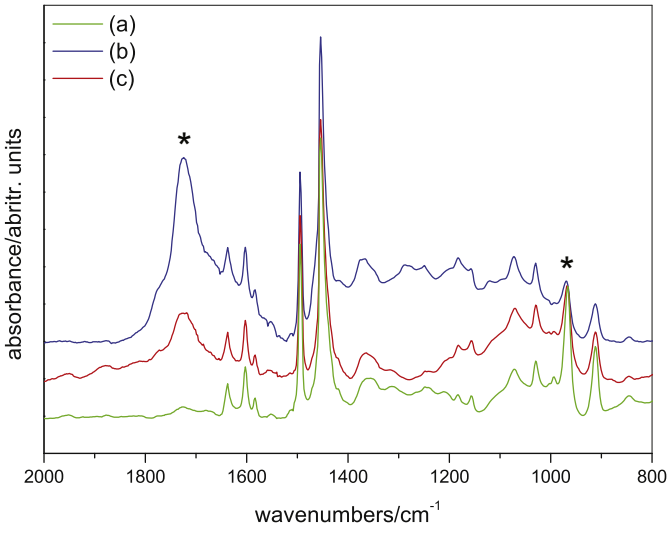

Fig. 9. FTIR spectra acquired from samples taken from three different areas from Grillo – (a) from the internal surface of the phone (Fig. 1B), (b) from the right side and (c) left side of the earpiece (Fig. 1A). Modifications in the C═O stretching are indicated with * (see frequencies in Supplementary information Table 1).

Acknowledgements

Authors wish to thank Arch. Davide Galletta for providing the Grillo telephone for study.

Appendix A. Supplementary data

Supplementary data related to this article can be found.

References

[1] Shashoua Y. Conservation of plastics: materials science, degradation and preservation. London: Routledge; 2008.
[2] Quye A, Williamson C, editors. Plastics, collecting and conserving. Edinburgh: NMS Publishing Limited; 1999.
[3] Lavédrine B, Fournier A, Martin G, editors. Preservation of plastic artefacts in museum collections. Paris: Éditions du Comité des travaux historiques et scientifiques; 2012.
[4] Lattuati-Derieux A, Egasse C, Thao-Heu S, Balcar N, Barabant G, Lavédrine B. What do plastics emit? HS—SPME—GC/MS analyses of new standard plastics and plastic objects in museum collections. J Cult Heritage 2013;14:238—47.
[5] Van den Broek WHAM, Derks EPPA, van de Ven EW, Wienke D, Geladi P, Buydens LMC. Chemometr Intell Lab 1996;35:187—97.
[6] Cséfalvayová L, Strlič M, Karjalainen H. Quantitative NIR chemical imaging in heritage science. Anal Chem 2011;83:5101—6.
[7] Pastorelli G, Trafela T, Taday PF, Portieri A, Lowe D, Fukunaga K, et al. Characterisation of historic plastics using terahertz time-domain spectroscopy and pulsed imaging. Anal Bioanal Chem 2012;403:1405—14.
[8] Htun T, Klein UKA. Laser-induced fluorescence decays of polyethylene films. J Lumin 2010;130:1275—9.
[9] Toja F, Saviello D, Nevin A, Comelli D, Lazzari M, Levi M, et al. The degradation of poly(vinyl acetate) as a material for design objects: a multi-analytical study of the effect of dibutyl phthalate plasticizer. Part 1. Polym Degrad Stab 2012;97(11):2441—8.
[10] Toja F, Saviello D, Nevin A, Comelli D, Lazzari M, Valentini G, et al. The degradation of poly(vinyl acetate) as a material for design objects: a multi-analytical study of the Cocoon lamps. Part 2, Polym Degrad Stab 2013;98(11):2215—23.
[11] Toja F, Nevin A, Comelli D, Levi M, Cubeddu R, Toniolo L. Fluorescence and Fourier-transform infrared spectroscopy for the analysis of iconic Italian design lamps made of polymeric materials. Anal Bioanal Chem 2011;399(9):2977—86.

[12] Davis P, Tiganis BE, Burn LS. The effect of photo-oxidative degradation on fracture in ABS pipe resins. Polym Degrad Stab 2004;84(2):233–42.
[13] Ghaemy M, Scott G. Photo-and thermal oxidation of ABS: correlation of loss of impact strength with degradation of the rubber component. Polym Degrad Stab 1981;3(3):233–42.
[14] Boldizar A, Möller K. Degradation of ABS during repeated processing and accelerated ageing. Polym Degrad Stab 2003;81(2):359–66.
[15] Santos RM, Botelho GL, Machado AV. Artificial and natural weathering of ABS. J Appl Polym Sci 2010;116:2005–14.
[16] Piton M, Rivaton A. Photo-oxidation of ABS at long wavelengths (lambda > 300 nm). Polym Degrad Stab 1997;55(2):147–57.
[17] Bokria JG, Schlick S. Spatial effects in the photodegradation of poly (acrylonitrile–butadiene–styrene): a study by ATR-FTIR. Polymer 2002;43(11): 3239–46.
[18] Jouan X, Gardette JL. Photo-oxidation of ABS: part 2—origin of the photodiscoloration on irradiation at long wavelengths. Polym Degrad Stab 1991;36(1):91–6.
[19] Blom H, Yeh R, Wojnarowski R, Ling M. Detection of degradation of ABS materials via OSC. Thermochim Acta 2006;442(1–2):64–6.
[20] Lala D, Rabek JF. The role of hydroperoxides in photo-oxidative degradation of cis-1,4-polybutadiene. Euro Polym J 1981;17(1):7–14.
[21] O'Connor DB, Scott GW. Emission spectra and kinetics of copolymer films of styrene and 2,3,4,5,6-pentafluorostyrene. Macromolecules 1991;24: 2355–60.
[22] David C, Zabeau F, Jacobs RA. Photo-oxidation and photo-stabilization of blends of low-density polyethylene and styrene–butadiene–styrene copolymers. Polym Eng Sci 1982;22(14):912–6.
[23] Luengo C, Allen NS, Edge M, Wilkinson A, Parellada MD, Barrio JA, et al. Photo-oxidative degradation mechanisms in styrene ethylene butadiene styrene (SEBS) triblock copolymer. Polym Degrad Stab 2006;91:947–56.
[24] Allen NS, Edge M, Wilkinson A, Liauw CM, Mourelatou D, Barrio J, et al. Degradation and stabilization of styrene–ethylene–butadiene–styrene (SEBS) block copolymer. Polym Degrad Stab 2001;71(1):113–22.
[25] Nevin A, Spoto G, Anglos D. Laser spectroscopies for elemental and molecular analysis in art and archaeology. Appl Phys A 2012;106(2):339–61.
[26] Comelli D, Nevin A, Valentini G, Osticioli I, Castellucci EM, Toniolo L, et al. Insights into Masolino's wall paintings in Castiglione Olona: advanced reflectance and fluorescence imaging analysis. J Cult Herit 2011;12(1):11–8.
[27] Comelli D, D'Andrea C, Valentini G, Cubeddu R, Colombo C, Toniolo L. Fluorescence lifetime imaging and spectroscopy as tools for nondestructive analysis of works of art. Appl Opt 2004;43(10):2175–83.
[28] Grahn H, Geladi P. Techniques and applications of hyperspectral image analysis. Chichester: John Wiley; 2007.
[29] http://www.tine.it/normal/UNINormal.htm [accessed 14.11.13].
[31] Comelli D, Valentini G, Nevin A, Farina A, Toniolo L, Cubeddu R. A portable UV-fluorescence multispectral imaging system for the analysis of painted surfaces. Rev Sci Inst 2008;79(8). art no. 086112.
[32] Bezdec JC. Pattern recognition with fuzzy objective function algorithms. New York: Plenum Press; 1981.
[33] Mailhot B, Gardette JL. Polystyrene photooxidation 1: identification of the IR absorbing photoproducts formed at short and long wavelengths. Macromolecules 1992;25(16):4119–26.
[34] Mailhot B, Gardette JL. Polystyrene photooxidation 2: a pseudo wavelength effect. Macromolecules 1992;25(16):4127–33.
[35] Basile LJ. Effect of styrene monomer on the fluorescence properties of polystyrene. J Chem Phys 1962;36(8):2204–10.
[36] Torkelson JM, Lipsky S, Tirrell M. Polystyrene fluorescence: effects of molecular weight in various solvents. Macromolecules 1981;14(5):1601–3.
[37] Healy MS, Hanson JE. Fluorescence excitation spectroscopy of polystyrene near the critical concentration c^*. J Appl Polym Sci 2007;104(1):360–4.